



# Predicting the current and future suitable distribution range of *Trilocho varians* (Walker, 1855) (Lepidoptera: Bombycidae) in China

Qianqian Qian\*, Danping Xu\*, Wenkai Liao and Zhihang Zhuo

College of Life Science, China West Normal University, Nanchong 637002, China

## Research Paper

\*These authors contributed equally to this work and should be regarded as co-first authors.

**Cite this article:** Qian Q, Xu D, Liao W, Zhuo Z (2024). Predicting the current and future suitable distribution range of *Trilocho varians* (Walker, 1855) (Lepidoptera: Bombycidae) in China. *Bulletin of Entomological Research* **114**, 317–326. <https://doi.org/10.1017/S0007485324000117>

Received: 20 July 2023  
Revised: 9 December 2023  
Accepted: 12 February 2024  
First published online: 3 May 2024

### Keywords:

climate change; environmental variables; MaxEnt model; potential geographical distribution; *Trilocho varians*

### Corresponding author:

Zhihang Zhuo;  
Email: [zhuozhihang@foxmail.com](mailto:zhuozhihang@foxmail.com)

## Abstract

*Trilocho varians* is one of the major pests of *Ficus* spp. Based on 19 bioclimatic variables provided by the Worldclim, our study analysed the suitable distribution areas of *T. varians* under current and future climate changes (SSP1-2.6, SSP2-4.5, SSP5-8.5) for two periods (the 2050s and 2090s) using the maximum entropy algorithm (MaxEnt) model. Key environmental variables affecting the geographic distribution of *T. varians* were also identified, and the changes in the area of suitable range under current and future climate changes were compared. The results showed that the key environmental variables affecting the distribution of *T. varians* were temperature and precipitation, comprising annual mean temperature (bio1), temperature seasonality (standard deviation  $\times$  100) (bio4), precipitation of driest month (bio14), and precipitation of driest quarter (bio17). Under the current climatic conditions, the suitable distribution area of *T. varians* is within the range of 92°13'E–122°08'E, 18°17'N–31°55'N. The current high, medium, and low suitable areas for *T. varians* predicted by the MaxEnt model are  $14.00 \times 10^4$ ,  $21.50 \times 10^4$ , and  $71.95 \times 10^4$  km<sup>2</sup>, of which the high suitable areas are mainly distributed in southern Guangdong, southwestern Guangxi, western Taiwan, Hong Kong, and Hainan. Under different future climatic conditions, some of the high, medium, and low suitability zones for *T. varians* increased and some decreased, but the mass centre did not migrate significantly. The Pearl River Basin is predicted to remain the main distribution area of *T. varians*.

## Introduction

*Trilocho varians* (Walker, 1855) is an insect of the family Bombycidae, that harms *Ficus* spp. Lepidoptera are holomorphic insects, so *T. varians* goes through four developmental stages common to holomorphic insects: eggs, larvae, pupae, and adults. *T. varians* is mainly distributed in South and Southeast Asian countries, such as Malaysia, Philippines, Vietnam, and Thailand. It is also widely distributed in southern China, especially in Taiwan and Hainan (Kedar *et al.*, 2014; Arya 2019). It is a major pest of *Ficus* spp. and its larvae cause 80–90% of *Ficus* spp. leaves to fall off (Kedar *et al.*, 2014). *Ficus* spp. that have been reported to have been damaged by *T. varians* include *Ficus elastica*, *Ficus benjamina*, *Ficus nitida*, *Ficus carraica*, *Ficus religiosa*, *Ficus infectoria*, *Ficus benghalensis*, and *Ficus septica* (Arya, 2019). *Ficus* spp. belongs to the family Moraceae with high ecological tolerance, high dispersal, and high germination rate, which is the reason why *Ficus* spp. as an exotic tree species in Macau, has become the main tree species for its parks (Zhang *et al.*, 2017). *Ficus* spp. is a native species of southern China, mainly in Taiwan, Zhejiang, Fujian, Guangdong, Guangxi, Guizhou, Yunnan, and other provinces, with trees up to 15–25 m in height and about 50 cm in diameter at breast height (Flora Reipublicae Popularis Sinicae, <http://www.cn-flora.ac.cn/>). *Ficus* spp. has an upright trunk, distinct shape, and fast growth rate, which can quickly increase the coverage of urban greenery, and its large canopy can also provide effective shade for pedestrians, so it is often used as an ornamental tree and street tree in landscape planning (Chen, 2020). At present, several papers have been published to describe the damage of *Ficus* spp. by *T. varians*. Basari *et al.* (2019) reported that *Ficus microcarpa* in Malaysia were attacked by *T. varians* larvae, resulting in 100% defoliation. Naeem-Ullah *et al.* (2020) reported that *F. microcarpa* leaves in Pakistan were heavily eaten by *T. varians*, which severely affected the ornamental value of *F. microcarpa*. Daimon *et al.* (2012) also documented that the larvae of *T. varians* affect two species of *Ficus*, *F. benjamina* and *F. microcarpa*, in Taiwan, China, and Okinawa, Japan. Therefore, research on the potential distribution range of *T. varians* is beneficial to the management and prevention of *Ficus* spp. pests and the maintenance of the urban greening environment.

In its sixth assessment report in 2022, the Intergovernmental Panel on Climate Change (IPCC) states that the Earth's average temperature has increased by 1.5°C from pre-industrial temperatures. Climate change is manifested in many ways, including increased temperatures

due to increased carbon dioxide concentrations, and extreme weather events such as droughts or storms (Jactel *et al.*, 2019). Rising sea levels, insecurity of food and water, and increased rates of transmission of infectious diseases under climate change pose a threat to human health and safety (Barrett *et al.*, 2015). Of course, global climate change not only threatens human survival but also affects other organisms. Climate change has already been reported to affect the body size of several contemporary species such as *Apodemus speciosus* and *Apodemus argenteus*, and may have an even greater impact on faunal communities in the future (Millien *et al.*, 2006). High temperatures increase insect mortality, and insect pheromone communication is disturbed by increased temperature and atmospheric gas concentrations (Boullis *et al.*, 2016). Climate change can also affect the distribution of insects. Climate change has been described to cause mountain butterflies to migrate to higher elevations (Rödger *et al.*, 2021). Local extinctions of bumblebees have been reported in extreme temperatures, and the risk of extinction will increase if climate change continues (Sirois-Delisle and Kerr, 2018). Climate change may reduce the abundance of Ephemeroptera, Plecoptera, and Trichoptera insects in temperate alpine regions of Switzerland (Timoner *et al.*, 2021). In conclusion, climate change has far-reaching effects on the geographical distribution of insects, and it is necessary to predict the geographical distribution of *T. varians* under future climate change to help us better prevent their infestation of *Ficus* spp.

Species distribution models (SDMs) are useful for predicting the future spatial distribution of species under changing climate scenarios and have been widely used in conservation biology, evolutionary biology, and biogeography (Islam *et al.*, 2021; Yang *et al.*, 2022a, 2022b). SDMs built using analytical methods such as climate change experiment, bioclimatic prediction system, generalised linear model, generalised additive model, ecological niche modelling, ecological niche factor analysis, genetic algorithm for rule-set prediction, and the maximum entropy algorithm (MaxEnt) have been widely used (Zhang *et al.*, 2021). The MaxEnt is a method for modelling species distributions when only species distribution data are available, and has been shown to perform well in predicting distribution (Sutton and Martin, 2022; Zhao *et al.*, 2022). Its accuracy and performance are higher than other models even with fewer distribution data (Aidoo *et al.*, 2022). At the same time, the MaxEnt model also has the advantages of short running time, easy operation, good performance, and high accuracy (He *et al.*, 2021). Among the existing investigations, Xu *et al.* (2022) predicted the suitable distribution area of *Oryctes rhinoceros* (L.) using the MaxEnt model. The results indicate that the MaxEnt model can be used for the research of suitable areas for insects. Similarly, Mugiyo *et al.* (2022) used the MaxEnt model to map the spatial distribution of underutilised crop species under climate change.

Despite its impact on *Ficus* spp., no studies have yet predicted the current and potential future distribution of *T. varians* using the MaxEnt model. In our report, MaxEnt was used to simulate the current potential distribution area of *T. varians* and to predict the potential distribution area of *T. varians* for two periods in the 2050s and 2090s under the three conditions of SSP1-2.6, SSP2-4.5, and SSP5-8.5 (shared socioeconomic pathways). The key environmental variables and suitable ranges affecting the distribution of *T. varians* were also analysed in conjunction with additional environmental variables. This study can help us to take appropriate control measures in advance to reduce the loss of *Ficus* spp. and advance the process of rational ecological research.

## Materials and methods

### Species occurrence data

Adequate occurrence records are an important prerequisite for the construction of species' ecological niche models (Li *et al.*, 2020). Three sources of occurrence records were used in this study, namely the Global Biodiversity Information Facility (<http://www.gbif.org/>), National Specimen Information Infrastructure (<http://www.nsii.org.cn/>), and literature related to *T. varians*. The related literature is from China National Knowledge Infrastructure (<https://www.cnki.net/>), but the occurrence records in the literature lack specific latitude and longitude coordinates, so we determined the coordinates of the occurrence records by Google Earth (<http://ditu.google.cn/>). Finally, a total of 122 occurrence records were obtained and saved in the .csv format for predictive modelling.

### Environmental variables

A total of 19 bioclimatic variables involved in this study were obtained from the Worldclim, and the data used in the modelling were based on meteorological records from 1970 to 2000. The IPCC, in its Fifth Assessment Report published in 2014, referred to the Representative Concentration Pathways (SSPs) being used in new climate model simulations. In this study, SSP1-2.6, SSP2-4.5, and SSP5-8.5 were selected to simulate the habitat suitability distribution of *T. varians* in the 2050s and 2090s, which represent three scenarios with different concentrations of greenhouse gas (GHG) emissions. Initial modelling was first performed using MaxEnt 3.4.4, and then the initial contribution of each environmental variable was calculated using the jackknife detection method, which eliminated mean temperature of coldest quarter (bio11), max temperature of warmest month (bio5), and precipitation of coldest quarter (bio19), the three variables with zero contribution. Then SPSS was used to calculate the Pearson correlation between the variables, and the variables with  $|p| > 0.8$  were removed. The combined contribution rate and Pearson correlation finally identified four environmental variables for re-modelling, namely annual mean temperature (bio1), temperature seasonality (standard deviation  $\times$  100) (bio4), precipitation of driest month (bio14), and precipitation of driest quarter (bio17).

### MaxEnt model building and evaluation

Re-modelling was performed based on the filtered dominant environment variables. The 25% of the occurrence records were randomly selected as the test set and the remaining 75% as the training set, and the computation was repeated ten times, with the replication run type set to 'cross-validation' and the maximum number of iterations set to 500. The receiver operating characteristic (ROC) curve is used to visualise the model performance, and the sum of the area under the curve (AUC value) is an important performance evaluation criterion to verify the accuracy of the model. The larger the AUC value, the greater the correlation between the environmental variables and the predicted geographical distribution of the species, and the better the prediction of the model (Zhang *et al.*, 2021). An AUC value of 0.5 means that the model is not better than random; an AUC value of  $<0.5$  means that the model is worse than random; an AUC value of 0.5–0.7 means that the model effect is weak; an AUC value of 0.7–0.9 means that the model effect is moderate; an AUC value of 0.9–1 means that the model effect is strong (Xu *et al.*, 2020). Afterwards, response curves were established to analyse the

response of *T. varians* to key environmental variables. According to the IPCC report, the probability of species presence (*P*) was divided into four classes, which were distinguished by different colours on the map: highly suitable ( $P \geq 0.66$ , red), moderately suitable ( $0.33 \leq P < 0.66$ , orange), weakly suitable ( $0.05 \leq P < 0.33$ , blue), and unsuitable ( $P < 0.05$ , green).

**Results**

*Model results validation*

With an AUC value of 0.970 (fig. 1), the model performed strongly and was accurate enough to be used to predict the geographic distribution of *T. varians*. Environmental variables with Pearson’s correlation  $|p| > 0.8$  were screened (table 1) and the contribution of these environmental variables was calculated using a Jackknife (table 2). Bio1 had a contribution rate of 59.6%, bio14 32.6%, bio4 6.4%, and bio17 1.4%. The cumulative contribution rate reached 100%, so these four environmental variables were finally selected for distribution modelling.

*The current distribution of T. varians*

The suitable potential distribution area for *T. varians* is divided into four classes, with green representing unsuitable areas, blue representing low suitable areas, orange representing medium suitable areas, and red representing high suitable areas (fig. 2). Under the current climatic conditions (table 3), the suitable distribution area of *T. varians* is within the range of 92°13'E–122°08'E, 18°17'N–31°55'N, mainly concentrated in low latitude and low altitude areas. The area of the high suitability zone is  $14.00 \times 10^4$  km<sup>2</sup>, accounting for 1.45% of the total area. It is mainly distributed in southern Guangdong, southwestern Guangxi, western Taiwan, Hong Kong, and the Hainan, and a small amount in southern Yunnan and southeastern Tibet. Most of these regions

**Table 1.** Results of Pearson correlation coefficient

	bio1	bio4	bio14	bio17
bio4	0.692**	1		
bio14	0.501**	0.428**	1	
bio17	0.512**	0.434**	0.594**	1

\*\*The difference is extremely significant at the 0.01 level ( $P < 0.01$ ).

**Table 2.** Contribution rate and permutation importance of each environment variables

Variable	Per cent contribution	Permutation importance
bio1	59.6	63.7
bio14	32.6	6
bio4	6.4	27.3
bio17	1.4	3

are located in the tropics and subtropics. Guangdong has the largest high suitability area of  $5.43 \times 10^4$  km<sup>2</sup>, followed by Guangxi and Hainan with  $2.89 \times 10^4$  and  $2.77 \times 10^4$  km<sup>2</sup>. The area of a highly suitable area in Hainan accounts for 78.27% of the total area of the province, the area of a highly suitable area in Taiwan accounts for 44.03% of the total area of the province, the area of a highly suitable area in Guangdong accounts for 30.21% of the total area of the province, and the area of a highly suitable area in Guangxi accounts for 12.14% of the total area of the province. Among them, the high suitability area of Hong Kong accounts for 82.07% of the total area, which is the most suitable area for the survival of *T. varians*. The area of the middle suitable zone is  $21.50 \times 10^4$  km<sup>2</sup>, accounting for 2.23% of the

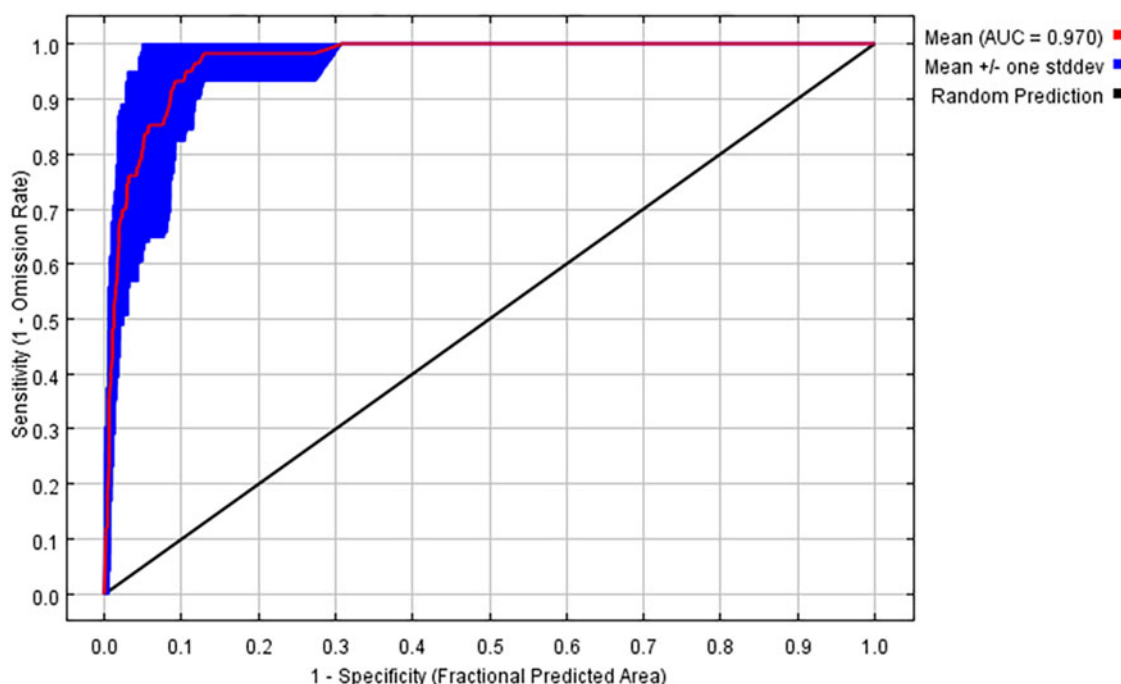


**Figure 1.** Area under the ROC curve (AUC) for *T. varians*.

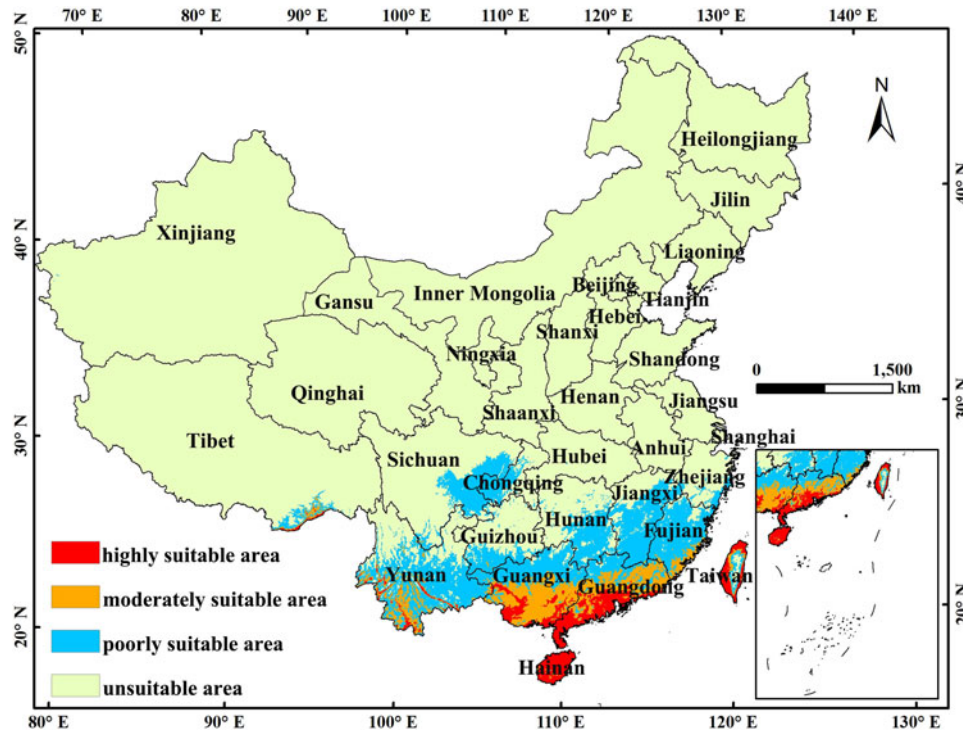


**Figure 2.** Current potential distribution of *T. varians*.

total area. It is mainly distributed in southern Guangdong and southern Guangxi, and a small amount is distributed in southern Yunnan and southern Fujian. The area of the low suitability zone is  $71.95 \times 10^4 \text{ km}^2$ , accounting for 7.47% of the total area. It is mainly distributed in Yunnan, Jiangxi, Fujian, southern Hunan, northern Guangxi, and northern Guangdong, and a small amount in Sichuan, Zhejiang, Tibet, and southern Guizhou. The rest are unsuitable areas, mainly distributed in northern China, such as Xinjiang, Inner Mongolia, Gansu, Hebei, Jilin, Heilongjiang, Liaoning, etc.

### Future distribution prediction of *T. varians*

In order to explore the impact of climate change on the distribution of *T. varians*, the potential distribution of three GHG

concentration scenarios, SSP1-2.6, SSP2-4.5, and SSP5-8.5, was simulated by the MaxEnt, and a total of six predictions were obtained for two periods (the 2050s and 2090s) (fig. 3). The results show (table 4) that in 2050s, under SSP1-2.6, the area of the high suitability zone is  $16.78 \times 10^4 \text{ km}^2$ , the medium suitability zone is  $17.56 \times 10^4 \text{ km}^2$ , and the low suitability zone is  $73.10 \times 10^4 \text{ km}^2$ . Under SSP2-4.5, the area of the high suitability zone is  $15.62 \times 10^4 \text{ km}^2$ , the medium suitability zone is  $19.79 \times 10^4 \text{ km}^2$ , and the low suitability zone is  $81.54 \times 10^4 \text{ km}^2$ . Under SSP5-8.5, the area of the high suitability zone is  $21.00 \times 10^4 \text{ km}^2$ , the medium suitability zone is  $18.77 \times 10^4 \text{ km}^2$ , and the low suitability zone is  $81.54 \times 10^4 \text{ km}^2$ . Under SSP5-8.5, the area of the high suitability area is  $21.00 \times 10^4 \text{ km}^2$ , the area of the medium suitability area is  $18.77 \times 10^4 \text{ km}^2$ , and the area of the low suitability area is  $74.53 \times 10^4 \text{ km}^2$ . Compared with the current distribution, the area

**Table 3.** Analysis of main suitable distributions of *T. varians*

Province	High suitable area ( $10^4 \text{ km}^2$ )	Total ( $10^4 \text{ km}^2$ )	Percentage of high suitable area in province	Percentage of high suitable area in China
Yunnan	0.91	39.41	2.32	0.10
Fujian	0.05	12.13	0.44	0.00
Guangxi	2.89	23.76	12.14	0.30
Taiwan	1.59	3.60	44.03	0.16
Guangdong	5.43	17.97	30.21	0.56
Hong Kong	0.09	0.11	82.07	0.01
Hainan	2.77	3.54	78.27	0.29
Tibet	0.27	122.84	0.22	0.03
China (land area)	14.00	960	-	1.45

of high suitability zones all increased, by 19.86, 11.57, and 50.64%, respectively. The area of medium suitability zones all decreased, by 18.33, 8.00, and 12.70%, respectively. The area of low suitability zones all increased, by 1.60, 13.33, and 3.59%, respectively. In

the 2090s, under SSP1-2.6, the area of the high suitability zone is  $11.67 \times 10^4 \text{ km}^2$ , medium suitability zone is  $17.88 \times 10^4 \text{ km}^2$ , and the low suitability zone is  $74.28 \times 10^4 \text{ km}^2$ . Under SSP2-4.5, the area of the high suitability zone is  $17.07 \times 10^4 \text{ km}^2$ , the medium

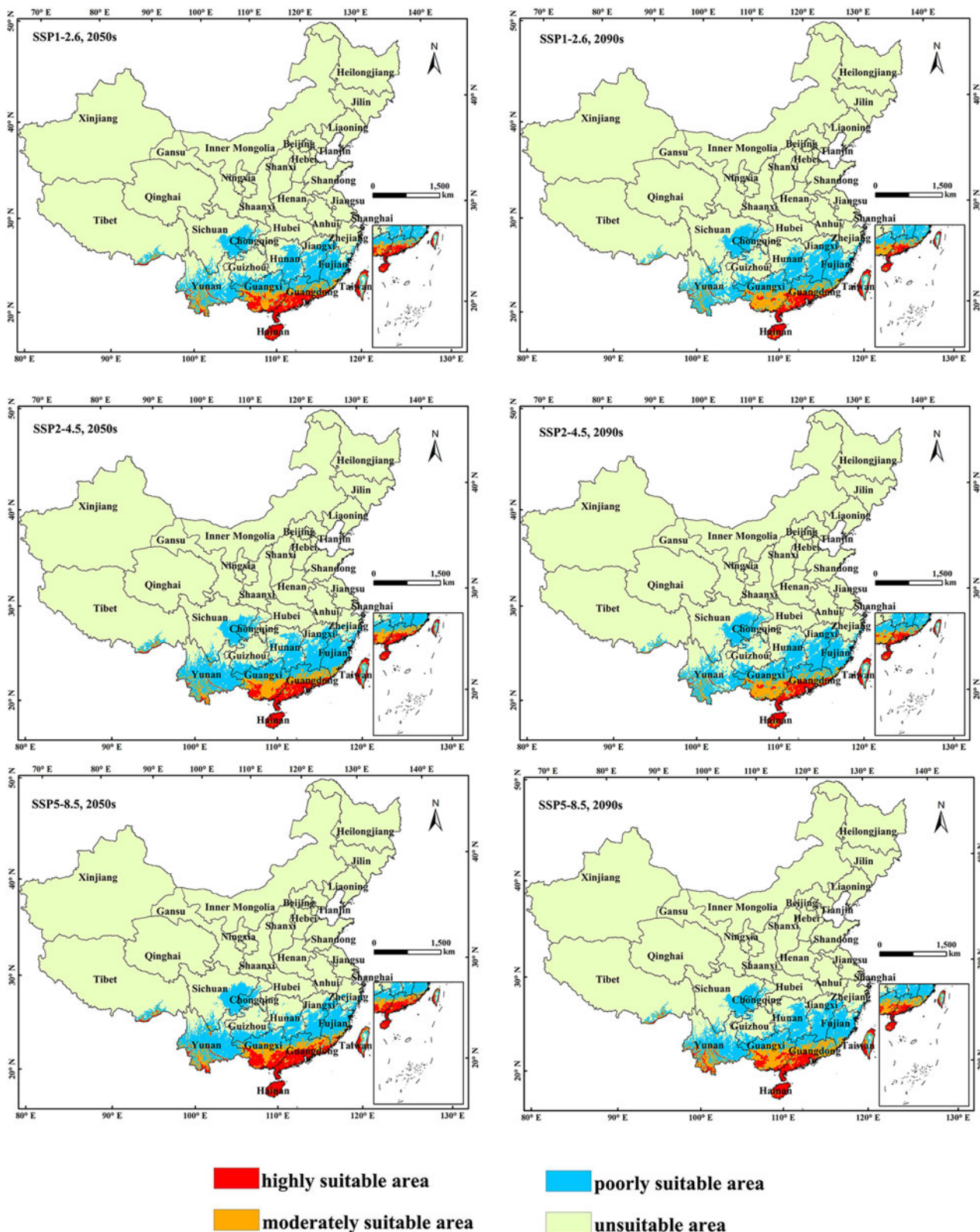


Figure 3. Future distribution of *T. varians*.

**Table 4.** Predicted suitable areas for *T. varians* under current and future climatic conditions

Decade	Scenarios	Predicted area (km <sup>2</sup> )			Comprise with current distribution (%)		
		High suitable area	Moderate suitable area	Low suitable area	High suitable area	Moderate suitable area	Low suitable area
Current	–	14.00	21.50	71.95	–	–	–
2050s	SSP1-2.6	16.78	17.56	73.10	19.86	–18.33	1.60
	SSP2-4.5	15.62	19.79	81.54	11.57	–8.00	13.33
	SSP5-8.5	21.09	18.77	74.53	50.64	–12.70	3.59
2090s	SSP1-2.6	11.67	17.88	74.28	–16.64	–16.84	3.24
	SSP2-4.5	17.07	17.75	76.37	21.93	–17.44	6.14
	SSP5-8.5	14.67	23.39	73.33	4.79	8.80	1.92

suitability zone is  $17.75 \times 10^4 \text{ km}^2$ , and the area of the low suitability zone is  $76.37 \times 10^4 \text{ km}^2$ . Under SSP5-8.5, the area of the high suitability zone is  $14.67 \times 10^4 \text{ km}^2$ , the area of the medium suitability zone is  $23.39 \times 10^4 \text{ km}^2$ , and the area of the low suitability zone is  $73.33 \times 10^4 \text{ km}^2$ . Compared to the current distribution, the area of the high suitability zone decreased by 16.64% under SSP1-2.6, increased by 21.93% under SSP2-4.5, and increased by 4.79% under SSP5-8.5. The area of the medium suitability zone decreased by 16.84% under SSP1-2.6, decreased by 21.93% under SSP2-4.5, and increased by 8.80% under SSP5-8.5. The area of low suitability zones all increased, by 3.24, 6.14, and 1.92%, respectively. Although the area of the suitable zone for *T. varians* increased and decreased under different conditions, the *T. varians* did not undergo significant migration.

Separate comparisons of changes in the area of high suitability areas showed that provinces with high suitability areas did not change in different periods and scenarios, only the area changed to different degrees (table 5). Yunnan had a substantial increase in the area of high suitability area under the SSP5-8.5 scenario in both periods, with an increase of 43.96 and 87.91%, respectively. In Fujian province, the area of high suitability area under the SSP5-8.5 scenario in the 2050s period increased substantially except for a large increase in the area of high suitability area under all other conditions. Guangxi showed an increase in all conditions except for a 60.21% decrease in the area of high

suitability area under the SSP1-2.6 scenario in the 2090s period. Taiwan, on the other hand, was the opposite of Guangxi, with only an increase of 11.95% under the SSP1-2.6 scenario in the 2090s. Guangdong decreased by 3.5% under the scenario of SSP5-8.5 in the 2090s, and the area of high suitability area increased under all other conditions. In Hong Kong, the area of high suitability area changed the most under the SSP5-8.5 scenario in the 2090s period, decreasing by 77.78%. Hainan had less change under all scenarios. The areas of high suitability areas in Tibet all showed an increase in the 2050s period and a decrease in the 2090s period. In terms of the total area of high suitability areas in China, the area increased under all scenarios except for the SSP5-8.5 scenario, which decreased by 16.64% in the 2090s.

#### Analysis of environmental variables

In order to identify key environmental variables that influence the potential distribution of *T. varians*, the regularised training gains of environmental variables were analysed by a jackknife. Among them (fig. 4), bio1 had the largest regularised training gain of more than 2.4, bio14 and bio17 had regularised training gains of less than 1.7, and bio4 had regularised training gains of less than 1.8. Meanwhile, these four environmental variables have a cumulative contribution of 100% and a cumulative permutation importance of 100%. Therefore, the most critical environmental

**Table 5.** Current and future changes in the size of high suitable areas for *T. varians*

Province	Current high suitable areas (10 <sup>4</sup> km <sup>2</sup> )	2050s comprise with current distribution (%)			2090s comprise with current distribution (%)		
		SSP1-2.6	SSP2-4.5	SSP5-8.5	SSP1-2.6	SSP2-4.5	SSP5-8.5
Yunnan	0.91	13.19	–31.87	43.96	–61.54	–28.57	87.91
Fujian	0.05	–80.00	–80.00	580.00	–100.00	–80.00	–100.00
Guangxi	2.89	54.33	18.67	114.88	–60.21	103.11	17.99
Taiwan	1.59	–12.58	–0.63	–13.21	11.95	–8.81	–18.24
Guangdong	5.43	23.20	24.13	55.25	10.13	11.23	–3.50
Hong Kong	0.09	–11.11	0	0	0	0	–77.78
Hainan	2.77	–18.05	0.36	2.17	–6.14	–1.44	–3.61
Tibet	0.27	29.63	40.74	85.19	–66.67	–11.11	–7.40
China	14.00	19.86	11.57	50.64	–16.64	21.93	4.79

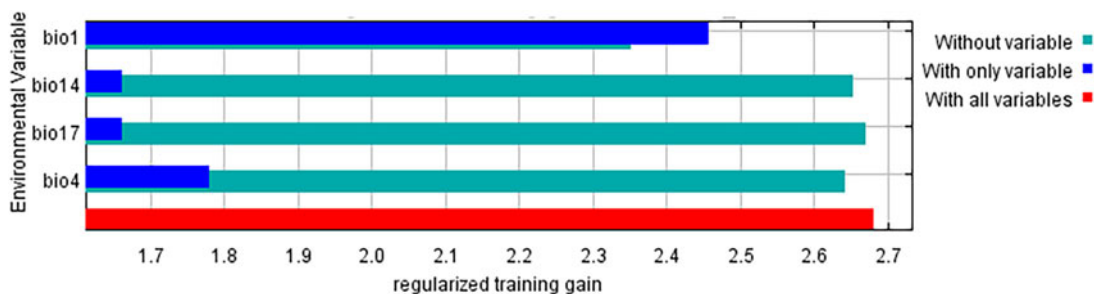


Figure 4. Importance of environment variables to *T. varians*.

variable affecting the geographical distribution of *T. varians* is the annual mean temperature (bio1), the temperature seasonality (standard deviation × 100) (bio4), the precipitation of driest month (bio14), and the precipitation of driest quarter (bio17). In other words, the temperature factor and precipitation factor had the most significant effect on the geographical distribution of *T. varians*. The optimum range of environmental variables affecting the geographical distribution of *T. varians* over a range was analysed by response curves (presence probability:  $P > 0.66$ ). The results showed (fig. 5) that the optimum range of annual mean temperature (bio1) was  $>20.50^{\circ}\text{C}$ , peaking at  $22.58^{\circ}\text{C}$ ; the temperature seasonality (standard deviation × 100) (bio4) was  $<554.17$ , peaking at  $234.67$ ; the precipitation of driest month

(bio14) was  $19.46\text{--}26.17$  and  $>58.79$  mm, peaking at  $22.73$  mm; the precipitation of driest quarter (bio17) was  $72.38\text{--}96.65$  and  $>264.98$  mm, peaking at  $86.36$  mm.

### Discussion

In this study, it was found that the distribution of *T. varians* was mainly influenced by four environmental factors: annual mean temperature (bio1), temperature seasonality (standard deviation × 100) (bio4), precipitation of driest month (bio14), and precipitation of driest quarter (bio17). The high suitability area of *T. varians* is mainly in the Pearl River Basin, and the suitability area will increase in the future, but the centre of mass did not undergo

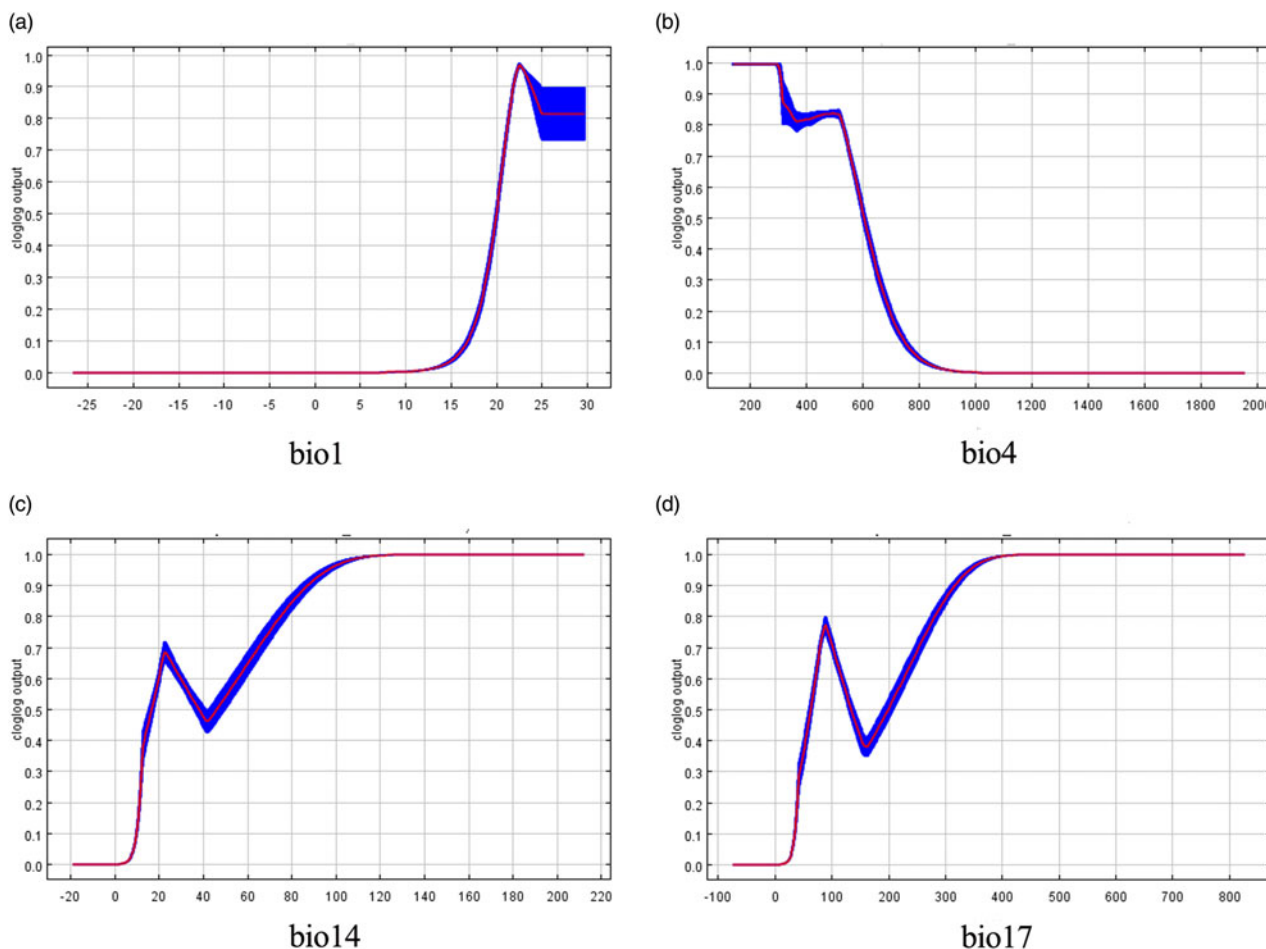


Figure 5. Response curve of environmental variables to occurrence probability of *T. varians*.

significant migration. Temperature and precipitation were found to be important environmental factors affecting the distribution of lepidopteran pests in previous articles of lepidopteran-related studies, e.g. *Spodoptera exigua* was affected by precipitation of the coldest quarter (bio19), annual precipitation (bio12) and mean temperature of the coldest quarter (bio11) (Falsafi *et al.*, 2022); *Zeuzera pyrina* was affected by precipitation of the coldest quarter (bio19), precipitation seasonality (bio15) and precipitation of driest quarter (bio17) (Fekrat and Farashi, 2022); the distribution of *Parapediasia teterrilla* was influenced by annual mean temperature (bio1), mean temperature of the coldest quarter (bio11), and precipitation of the coldest quarter (bio19) (Jie *et al.*, 2020). Temperature and precipitation were equally key environmental variables in this study. The suitable distribution area for *T. varians* is in the Pearl River Basin (102°14'E–115°53'E; 21°31'N–26°49'N), which has a tropical monsoon climate and a subtropical monsoon climate (Gu *et al.*, 2016; Zhang *et al.*, 2021). The tropical monsoon climate is characterised by year-round hot temperatures above 20°C and annual precipitation of 1500–2000 mm. (Wu *et al.*, 2008). The average annual temperature in the subtropical monsoon climate zone ranges from 15 to 22°C, and annual precipitation ranges from 800 to 1600 mm (Wu *et al.*, 2008). In the existing studies, 24–26°C and 60.5% relative humidity are usually chosen for selection and cultivation of *T. varians*, indicating that it is suitable for survival under these conditions (Basari *et al.*, 2019; Ramzan, 2020). The results of this paper show that the optimal range of annual average temperature (bio1) suitable for *T. varians* is greater than 20.50°C, the precipitation of driest month (bio14) >58.79 mm, and the precipitation of driest quarter (bio17) >264.98 mm. Temperature and precipitation in subtropical and tropical monsoon climates also fall within this range. Meanwhile, the results demonstrated that *T. varians* is completely unsuitable in northeast, north, and northwest China. This may be related to the local temperature and precipitation, for example, northwest China has a continental arid climate where the temperature can reach below –30°C in the coldest months and the annual precipitation is 100–200 mm (Yang *et al.*, 2022a, 2022b). Comparison of the topographic map of China provided by the Chinese government website with the predictions of our survey revealed that *T. varians* is mainly distributed at low elevations and low latitudes, such as Guangdong, Guangxi, and Hainan. These places are all below 200 m in elevation, below 30°N in latitude, with abundant precipitation and high mean annual temperatures (Wu *et al.*, 2008). This indicates that *T. varians* does not have good environmental adaptability and can only survive in areas with suitable precipitation and temperature.

Under different future climatic conditions, some of the high, medium, and low suitability zones for *T. varians* increased and some decreased. The total suitable zone showed an increase, but not significant. *T. varians* is mainly distributed in the Pearl River Basin. It is reported that the monthly mean temperature in the Pearl River Basin will increase by 0.25–0.34°C per decade under RCP4.5 and by 0.42–0.60°C per decade under SSP5-8.5, and the mean annual precipitation will also increase under both RCPs (Duan *et al.*, 2020). However, under RCP4.5, drought events lasting 3–4 months will increase by 4.3% and those lasting more than 5 months will increase by 3.4%. Under RCP8.5, more medium- and long-term drought events with higher severity will occur (Zhou *et al.*, 2021). In CMIP6, new scenario shared economy paths (SSPs) were developed that integrate CMIP5 representative centralised paths (RCPs), so the results can be used to

some extent as a reference to explain the findings of this paper (Hirsch *et al.*, 2018). The results of our study showed that the area of most of the high and low suitability zones for *T. varians* increased under future climatic conditions, which may be related to the increase of temperature and precipitation in the future. At the same time, the medium suitability zones mostly decreased, which may be related to the increase in drought duration.

The increase in the area of high, medium, and low suitability areas for *T. varians* in most future scenarios suggests that future environmental conditions will be more favourable for *T. varians* to survive and reproduce. Logan *et al.* (2007) modelled future climate change and found that warming favours the reproduction and survival of *Lymantria dispar*, while its colonisation of poplar will increase from 33% in 1991 to 100% in 2071. Hodkinson (1997) found that the host range of *Cacopsylla groenlandica* expanded from one species of willow to four species of willow due to climate warming. Therefore, it is hypothesised that changes in the distribution area of *T. varians* may result in increased damage to *Ficus* spp. or more *Ficus* spp. species being infested.

The MaxEnt model is highly accurate for species distribution prediction but still differs from reality. In the current work, we chose environmental variables from meteorological records from 1970 to 2000, but global climate change has been dramatic in recent years. The IPCC mentioned in the second part of its Sixth Assessment Report that global warming will exceed 1.5 or 2°C during the 21st century, and that there are large uncertainties in the conversion of emission scenarios into concentration pathways due to uncertainties in climate-carbon cycle feedbacks. The average precipitation will also increase, but with seasonal and regional variability, with an increase in synoptic variability (Zhuo *et al.*, 2020). Therefore, the environmental variables used in this study may differ significantly from those under future climate change. Also, the factors affecting the distribution of species are multiple. Human activities affect the distribution of species, and the distribution of plants fed on by phytophagous insects also affects the distribution of insects (Qin *et al.*, 2020; Yang *et al.*, 2022a, 2022b). In this study, we only considered the effects of 19 environmental variables on the distribution of *T. varians*. We did not explore whether there is a link between the distribution area of *Ficus* spp. and the potential distribution of *T. varians*. However, our report can still explain to some extent the suitable distribution area of *T. varians* and provide reference value for controlling it.

## Conclusions

In this work, the currently suitable areas for *T. varians* were analysed using the MaxEnt model, and key environmental variables affecting the distribution of *T. varians* were identified. The potential distribution of *T. varians* was predicted under three concentration pathways, SSP1-2.6, SSP2-4.5, and SSP5-8.5, for the periods of 2050s and 2090s, respectively. The research concluded that the current high, medium, and low suitability zones of *T. varians* predicted by the MaxEnt model accounted for 1.45, 2.23, and 7.47% of the total land area of China, respectively, and were mainly distributed in Guangdong, Guangxi, Hainan, Taiwan, and Hong Kong. The annual mean temperature (bio1), the temperature seasonality (standard deviation × 100) (bio4), the precipitation of driest month (bio14), and the precipitation of driest quarter (bio17) are the key environmental variables affecting the geographical distribution of *T. varians*. Under future climate change, the geographic distribution of *T. varians* did not



shift significantly and remained concentrated in Guangxi, Guangdong, Hainan, Taiwan, and Hong Kong.

### Availability of data and material

The data supporting the results are available in a public repository at: GBIF.org (5 June 2022) GBIF Occurrence Download <https://doi.org/10.15468/dl.7dsrcm9> and Qianqian Qian (2024): Locations of *Trilocha varians* figshare dataset. <https://doi.org/10.6084/m9.figshare.25133168.v1>.

**Author contributions.** Qianqian Qian and Zhihang Zhuo: conceptualisation; Danping Xu: methodology; Zhihang Zhuo: software; Wenkai Liao: investigation; Qianqian Qian: writing – original draft; Zhihang Zhuo: writing – review and editing. All authors have read and agreed to the published version of the manuscript.

**Financial support.** This research was funded by Sichuan Province Science and Technology Support Program (2022NSFSC0986), China West Normal University Support Program (20A007, 20E051, 21E040, and 22ka011).

**Competing interests.** None.

### References

- Aidoo O, Souza PG, Silva R, Santana Júnior P, Picanço M, Osei-owusu J, Setamou M, Ekesi S and Borgemeister C (2022) A machine learning algorithm-based approach (MaxEnt) for predicting invasive potential of *Trioza erytreae* on a global scale. *Ecological Informatics* 71, 101792.
- Arya P (2019) Recent Diversity and Potentia Biological Control Studies on Major Ornamental *Ficus* sp. Defoliating Moth Bombycid *Trilocha* (= *Ocinara*) *variens* (Walker) (Lepidoptera: Bombycidae).
- Barrett B, Charles JW and Temte JL (2015) Climate change, human health, and epidemiological transition. *Preventive Medicine* 70, 69–75.
- Basari N, Mustafa N, Yusrihan N, Chin W and Ibrahim Z (2019) The effect of temperature on the development of *Trilocha varians* (Lepidoptera: Bombycidae) and control of the *Ficus* plant pest. *Tropical Life Sciences Research* 30, 23–31.
- Boullis A, Detrain C, Francis F and Verheggen F (2016) Will climate change affect insect pheromonal communication? *Current Opinion in Insect Science* 17, 87–91.
- Chen S (2020) Application and suitable planting of *Ficus microcarpa* in urban greening. *Guangdong Landscape Architecture* 42, 55–58.
- Daimon T, Yago M, Hsu Y, Fujii T, Nakajima Y, Kokusho R, Abe H, Katsuma S and Shimada T (2012) Molecular phylogeny, laboratory rearing, and karyotype of the bombycid moth, *Trilocha varians*. *Journal of Insect Science (Online)* 12, 49.
- Duan R, Huang G, Li Y, Zhou X, Ren J and Tian C (2020) Stepwise clustering future meteorological drought projection and multi-level factorial analysis under climate change: a case study of the Pearl River Basin, China. *Environmental Research* 196, 110368.
- Falsafi H, Alipanah H, Ostovan H, Hesami S and Zahiri R (2022) Forecasting the potential distribution of *Spodoptera exigua* and *S. littoralis* (Lepidoptera, Noctuidae) in Iran. *Journal of Asia-Pacific Entomology* 25, 101956.
- Fekrat L and Farashi A (2022) Impacts of climatic changes on the worldwide potential geographical dispersal range of the leopard moth, *Zeuzera pyrina* (L.) (Lepidoptera: Cossidae). *Global Ecology and Conservation* 34, e2050.
- Gu X, Qiang Z, Vijay S and Peijun S (2016) Hydrological response to large-scale climate variability across the Pearl River Basin, China: spatio-temporal patterns and sensitivity. *Global and Planetary Change* 149, 1–13.
- He P, Li J, Li Y, Xu N, Gao Y, Guo L, Huo T, Peng C and Meng F (2021) Habitat protection and planning for three Ephedra using the MaxEnt and Marxan models. *Ecological Indicators* 133, 108399.
- Hirsch A, Guilloid B, Seneviratne S, Beyerle U, Boysen L, Brovkin V, Davin E, Doelman J, Kim H, Mitchell D, Nitta T, Shiogama H, Sparrow S, Stehfest E, Vuuren D and Wilson S (2018) Biogeophysical impacts of land-use change on climate extremes in low-emission scenarios: results from HAPPI-land. *Earth's Future* 6, 396–409.
- Hodkinson ID (1997) Progressive restriction of host plant exploitation along a climatic gradient: the willow psyllid *Cacopsylla groenlandica* in Greenland. *Ecological Entomology* 22, 47–54.
- Islam KN, Rana LRS, Islam K, Hossain MS, Hossain MM and Hossain MA (2021) Climate change and the distribution of two *Ficus* spp. in Bangladesh – predicting the spatial shifts. *Trees, Forests and People* 4, 100086.
- Jactel H, Koricheva J and Castagneyrol B (2019) Responses of forest insect pests to climate change: not so simple. *Current Opinion in Insect Science* 35, 103–108.
- Jie L, Yang J and Li W (2020) Potential distribution analysis of an invasive alien species *Parapediasia teterrella* (Lepidoptera, Crambidae) in East Asia. *Journal of Asia-Pacific Entomology* 23, 219–223.
- Kedar SC, Mallalath K and Saini R (2014) First report of *Trilocha* (= *Ocinara*) *variens* and its natural enemies on *Ficus* spp. from Haryana, India. *Journal of Entomology and Zoology Studies* 2, 268–270.
- Li X, Xu D, Jin Y, Zhuo Z, Yang H, Hu J and Wang R (2020) Predicting the current and future distributions of *Brontispa longissima* (Coleoptera: Chrysomelidae) under climate change in China. *Global Ecology and Conservation* 25, e1444.
- Logan J, Regniere J, Gray D and Munson S (2007) Risk assessment in the face of a changing environment: gypsy moth and climate change in Utah. *Ecological Applications: A Publication of the Ecological Society of America* 17, 101–117.
- Millien V, Lyons S, Olson L, Smith F, Wilson A and Yom-Tov Y (2006) Ecotypic variation in the context of global climate change: revisiting the rules. *Ecology Letters* 9, 853–869.
- Mugiyo H, Chimonyo V, Kunz R, Sibanda M, Nhamo L, Masemola C, Modi A and Mabhaudhi T (2022) Mapping the spatial distribution of underutilised crop species under climate change using the MaxEnt model: a case of KwaZulu-Natal, South Africa. *Climate Services* 28, 100330.
- Naeem-Ullah U, Ramzan M, Saeed S, Iqbal N, Umar U, Sarwar Z, Ali M, Saba S, Abid A, Khan K and Ghranh H (2020) Toxicity of four different insecticides against *Trilocha varians* (Bombycidae: Lepidoptera). *Journal of King Saud University - Science* 32, 1853–1855.
- Qin A, Jin K, Batsaikhan M, Nyamjav J, Li G, Jia L, Xue Y, Sun G, Wu L, Indree T, Shi Z and Xiao W (2020) Predicting the current and future suitable habitats of the main dietary plants of the Gobi bear using MaxEnt modeling. *Global Ecology and Conservation* 22, e1032.
- Ramzan M (2020) Effect of temperature on the life cycle of *Trilocha varians* (Lepidoptera: Bombycidae) in Pakistan. *Pure and Applied Biology* 9, 436–442.
- Rödger D, Schmitt T, Gros P, Ulrich W and Habel J (2021) Climate change drives mountain butterflies towards the summits. *Scientific Reports* 11, 12021–14382.
- Sirois-Delisle C and Kerr J (2018) Climate change-driven range losses among bumblebee species are poised to accelerate. *Scientific Reports* 8, 1–10.
- Sutton GF and Martin GD (2022) Testing MaxEnt model performance in a novel geographic region using an intentionally introduced insect. *Ecological Modelling* 473, 110139.
- Timoner P, Fasel M, AshrafVaghefi S, Marle P, Castella E, Moser F and Lehmann A (2021) Impacts of climate change on aquatic insects in temperate alpine regions: complementary modeling approaches applied to Swiss rivers. *Global Change Biology* 27, 3565–3581.
- Wu G, Wang N, Hu S, Tian L and Tian J (2008) *Physical Geography*. Beijing, China: Higher Education Press.
- Xu D, Li X, Jin Y, Zhuo Z, Yang H, Hu J and Wang R (2020) Influence of climatic factors on the potential distribution of pest *Heortia vitessoides* Moore in China. *Global Ecology and Conservation* 23, e1107.
- Xu D, Zhuo Z, Li X and Wang R (2022) Distribution and invasion risk assessment of *Oryctes rhinoceros* (L.) in China under changing climate. *Journal of Applied Entomology* 146, 385–395.
- Yang J, Huang Y, Jiang X, Chen H, Liu M and Wang R (2022a) Potential geographical distribution of the endangered plant isoetes under human activities using MaxEnt and GARP. *Global Ecology and Conservation* 38, e2186.
- Yang L, Wen X, Barzegar R, Adamowski J, Meng Z and Yin Z (2022b) Contributions of climate, elevated atmospheric CO<sub>2</sub> concentration and

- land surface changes to variation in water use efficiency in Northwest China. *Catena* **213**, 106220.
- Zhang H, Lai PY and Jim CY** (2017) Species diversity and spatial pattern of old and precious trees in Macau. *Landscape and Urban Planning* **162**, 56–67.
- Zhang S, Liu X, Li R, Wang X, Cheng J, Yang Q and Kong H** (2021) AHP-GIS and MaxEnt for delineation of potential distribution of Arabica coffee plantation under future climate in Yunnan, China. *Ecological Indicators* **132**, 108339.
- Zhao Z, Xiao N, Shen M and Li J** (2022) Comparison between optimized MaxEnt and random forest modeling in predicting potential distribution: a case study with *Quasipaa boulengeri* in China. *Science of the Total Environment* **842**, 156867.
- Zhou T, Chen Z and Xiao L** (2021) Interpreting IPCC AR6: future global climate based on projection under scenarios and on near-term information. *Advances in Climate Change Research* **17**, 652–663.
- Zhuo Z, Xu D, Pu B, Wang R and Ye M** (2020) Predicting distribution of *Zanthoxylum bungeanum* Maxim. in China. *BMC Ecology* **20**, 46.